# A Fluorescent Molecular Switch Driven by the Input Sequence of Metal Cations: An Azamacrocyclic Ligand Containing Bipolar Anthracene Fragments

## Go Nishimura, Hajime Maehara, Yasuhiro Shiraishi,* and Takayuki Hirai[a]

**Abstract:** An azamacrocyclic ligand (**L**) containing two anthracene (AN) fragments connected through two triethylenetetramine bridges has been synthesized, in which each of the bridges can coordinate with one metal cation. The effects of pH and metal cations ($Zn^{2+}$ and $Cd^{2+}$) on the emission properties of **L** were studied in water. Without metal cations, **L** does not show any emission at basic pH values. The addition of $Zn^{2+}$ leads to the production of excimer emission, which is due to a static excimer formed by direct excitation of the intramolecular ground-state dimer of the bipolar AN fragments that approach each other by $Zn^{2+}$ binding. In contrast, $Cd^{2+}$ addition does not result in excimer emission because the $Cd^{2+}$–AN π complex, formed by donation of a π electron of the AN fragments to the adjacent $Cd^{2+}$, suppresses π-stacking interactions of the AN fragments. The most notable feature is the appearance of excimer emission controlled by the input sequence of metal cations: $Zn^{2+} \rightarrow Cd^{2+}$ sequential addition (each one equivalent) allows excimer emission, whereas the reverse sequence ($Cd^{2+} \rightarrow Zn^{2+}$) does not. In the $Zn^{2+} \rightarrow Cd^{2+}$ sequence, $Cd^{2+}$ coordination is structurally restricted by the first $Zn^{2+}$ coordination with the other polyamine bridge, leading to the formation of a weak $Cd^{2+}$–AN π complex. In contrast, for the reverse sequence, the first $Cd^{2+}$ coordination forms a stable $Cd^{2+}$–AN π complex, which is not weakened by sequential $Zn^{2+}$ coordination, resulting in no excimer emission.

**Keywords:** anthracene · cations · excimers · fluorescence · molecular switches

## Introduction

The design of supramolecular systems whose optical or electronic properties can be modulated by external stimuli is an area of intense research activity.[1] In particular, molecular systems that perform as elementary electronic devices are of tremendous significance to the development of miniaturized device components. The potential application of these components in optical and electronic memory devices has attracted considerable effort to this research area.[2] Of particular interest is the design of fluorescent molecular switches, as they can precisely control the fluorescence properties by simple chemical input, even down to the level of single molecules or ions under ambient conditions.[3] Various molecular switches have been proposed based on systems whose emission properties can be modulated by external inputs, such as temperature,[4] light,[5] redox potential,[6] and ions.[7] Metal cations are often used as the input chemicals because the metal cation binding often triggers several photoinduced processes, such as electron transfer,[3a,8] charge transfer,[3a,9] and energy transfer,[10] thus enabling the modulation of emission properties. However, most of these are driven by a single metal-cation input.[11] Recently, more integrated switches, driven by a combination of multiple metal cation inputs, have been proposed.[12] However, a system in which the "sequence" of metal cation inputs changes the emission properties had not been proposed.

In this work, we synthesized a simple azamacrocyclic ligand (**L**) with two anthracene (AN) fragments connected through two triethylenetetramine bridges (Scheme 1), in which each of the bridges can coordinate with one metal cation. The effects of pH and metal cations ($Zn^{2+}$ and $Cd^{2+}$) on the emission properties were studied in water. We found that $Zn^{2+}$ coordination with **L** leads to the production of excimer emission, which is due to a static excimer formed by direct excitation of the intramolecular ground-state dimer

[a] Dr. G. Nishimura, H. Maehara, Dr. Y. Shiraishi, Prof. T. Hirai
Research Center for Solar Energy Chemistry
and Division of Chemical Engineering
Graduate School of Engineering Science
Osaka University
Toyonaka 560-8531 (Japan)
Fax: (+81)6-6850-6271
E-mail: shiraish@cheng.es.osaka-u.ac.jp
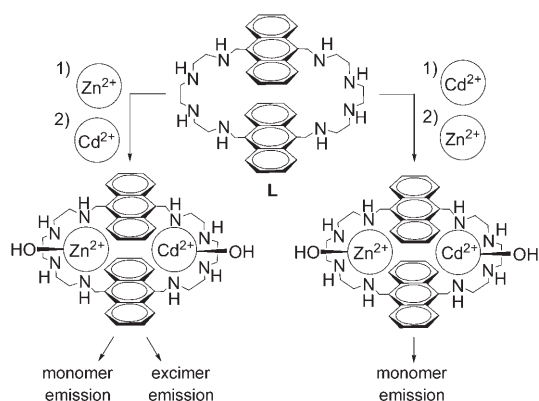
Scheme 1. Schematic representation of excimer emission switching of **L** driven by the input sequence of metal cations.



Figure 1. A) pH-dependent change in fluorescence intensity ($I$; $\lambda_{ex} =$ 368 nm; 298 K) of **L** (50 μM) in aqueous NaClO$_4$ (0.15 M) solution without metal cations. B) pH-dependent change in $I_M$ (monitored at 420 nm, ○) and mole fraction distribution of different **L** species (-----), in which H$_8$L$^{8+}$ and H$_7$L$^{7+}$ species and HL$^+$ and fully deprotonated **L** species are shown as their total quantities. Each spectrum in A) corresponds to the plots in B).

(GSD) of the bipolar AN fragments that approach each other by Zn$^{2+}$ coordination. In contrast, Cd$^{2+}$ addition does not result in excimer emission because the Cd$^{2+}$–AN π complex, formed by donation of a π electron of the AN fragments to the adjacent Cd$^{2+}$ center, suppresses formation of the GSD. The most notable feature of **L** is the effects of the input sequence of metal cations (Scheme 1): Zn$^{2+}$→Cd$^{2+}$ sequential addition (one equivalent each to **L**) allows excimer emission, whereas the reverse sequence (Cd$^{2+}$→Zn$^{2+}$) does not. To the best of our knowledge, this is the first molecular switch driven by the input sequence of chemicals. We report here that this unprecedented excimer emission switching is driven by a stability difference of the Cd$^{2+}$–AN π complex, which is directed by the metal cation that is added first.

## Results and Discussion

**Synthesis**: Ligand **L** was readily synthesized in a manner similar to the azamacrocyclic ligand containing two AN fragments connected through two diethylenetriamine bridges.[13] Anthracene-9,10-dicarbaldehyde and triethylenetetramine were stirred in a mixture of CH$_3$CN/CH$_3$OH at 323 K. The resultant solution was treated with NaBH$_4$ in CH$_3$OH at 323 K. The raw material obtained was purified by precipitation with a concentrated aqueous HCl solution in ethanol followed by recrystallization in diethyl ether/ethanol, affording **L** as a brown powder in 20% yield.

**Effect of pH**: The emission properties of **L** without metal cations were studied first. Figure 1A shows the pH-dependent change in the fluorescence spectra of **L** measured in water ($\lambda_{ex} =$ 368 nm). Ligand **L** shows a distinctive fluorescence at 380–500 nm, assigned to a monomer emission from the locally excited AN fragment. Figure 1B plots the intensity of the monomer emission ($I_M$) monitored at 420 nm against pH, for which the dashed lines denote the mole fraction distribution of the different **L** species, which is calculated from the protonation constants determined potentiometrically (Table 1). The $I_M$ is strong at acidic pH values, but de-
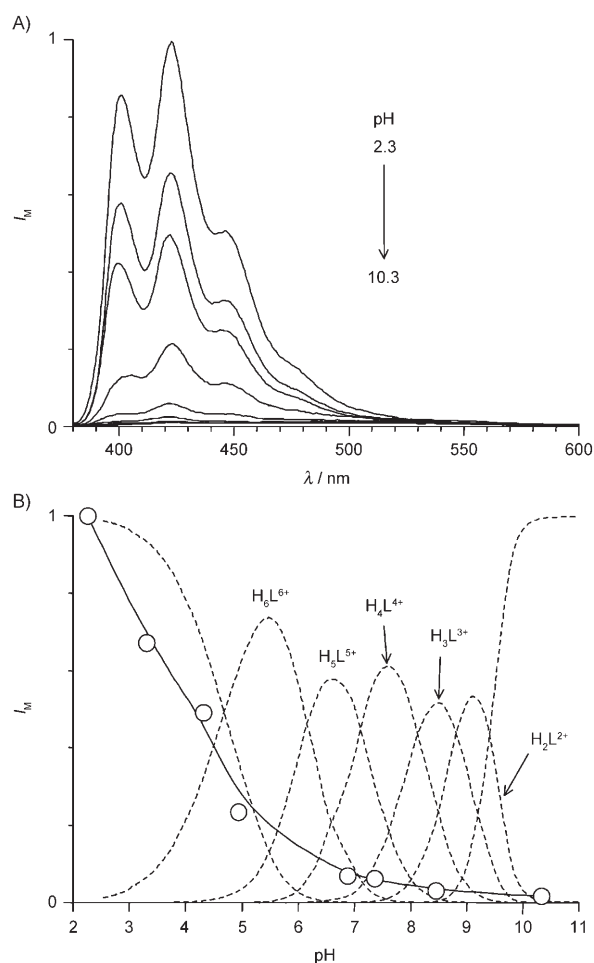
creases with increasing pH and becomes almost zero at pH > 7. As is also observed for related AN-conjugated polyamines,[14] this $I_M$ decrease is because the deprotonation of the nitrogen atoms of **L**, associated with a pH increase, leads to electron transfer (ET) from the unprotonated nitrogen atoms to the photoexcited AN monomer, resulting in

Table 1. Logarithms of the protonation constants of **L** determined in aqueous NaClO$_4$ (0.15 M) solution at 298 K.

| Reaction[a] | |
| --- | --- |
| 2H + L → H$_2$L | 18.79 ± 0.07 |
| H + H$_2$L → H$_3$L | 8.81 ± 0.07 |
| H + H$_3$L → H$_4$L | 8.14 ± 0.08 |
| H + H$_4$L → H$_5$L | 7.08 ± 0.08 |
| H + H$_5$L → H$_6$L | 6.17 ± 0.08 |
| H + H$_6$L → H$_7$L | 4.70 ± 0.08 |
| log β | 53.68 |

[a] Charges are omitted for clarity.

quenching of the excited AN monomer. Figure 2A shows the absorption spectra of **L**; the spectra scarcely differ over the entire pH range. As shown in Figure 2B, the excitation spectra of **L** collected at 420 nm are similar to the absorption spectra.
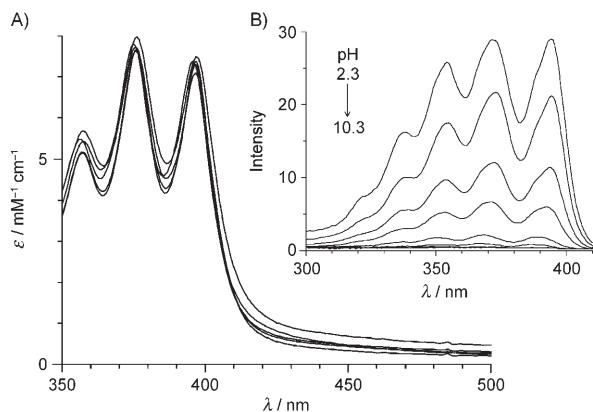


Figure 2. pH-dependent change in A) absorption and B) excitation spectra collected at 420 nm (monomer emission) of **L** (50 μM) in aqueous NaClO$_4$ (0.15 M) solution without metal cations (298 K). Each of the spectra corresponds to the plots in Figure 1B.

**Effect of Zn$^{2+}$ addition**: Figure 3A shows the pH-dependent change in the emission spectra of **L** measured with two equivalents of Zn$^{2+}$. Figure 3B (open symbols) plots the change in $I_M$ with pH, for which the dashed lines denote the mole fraction distribution of the species, which is calculated from the protonation and stability constants determined potentiometrically (Tables 1 and 2). The $I_M$ decreases with increasing pH, but is constant at pH > 7 (at 90% decreased level), whereas the absence of Zn$^{2+}$ shows almost zero $I_M$ at pH > 7 (Figure 1B). As is also observed for related AN-conjugated polyamines,[15] the appearance of monomer emission at basic pH is due to the decrease in electron density of the nitrogen atoms of the polyamine bridges through Zn$^{2+}$ coordination, which suppresses ET from the nitrogen atoms to the excited AN fragment. A notable feature of **L** inspired by the addition of Zn$^{2+}$ is the appearance of a red-shifted emission at 450–600 nm, assigned to an intramolecular excimer formed between the bipolar AN fragments that approach each other by Zn$^{2+}$ coordination.[14a] As shown in Figure 3B (filled symbols), the intensity of this excimer emission ($I_E$) monitored at 500 nm increases at pH > 7, for which the increase corresponds to the formation of OH$^-$-coordinated [Zn$_2$L(OH)]$^{3+}$ and [Zn$_2$L(OH)$_2$]$^{2+}$ species.

Figure 4A shows the pH-dependent change in the absorption spectra of **L** measured with two equivalents of Zn$^{2+}$. The absorbance of **L** at > 400 nm "rises" with the pH increase in the range of 4–7, for which OH$^-$-free Zn$^{2+}$–**L** complexes ([Zn$_2$H$_2$L]$^{6+}$, [Zn$_2$HL]$^{5+}$, and [Zn$_2$L]$^{4+}$) exist (Figure 3B). With Zn$^{2+}$, no precipitation occurs at any pH value, and filtration of the solution does not lead to any change in $I_M$, $I_E$, and absorption spectra. In addition, the
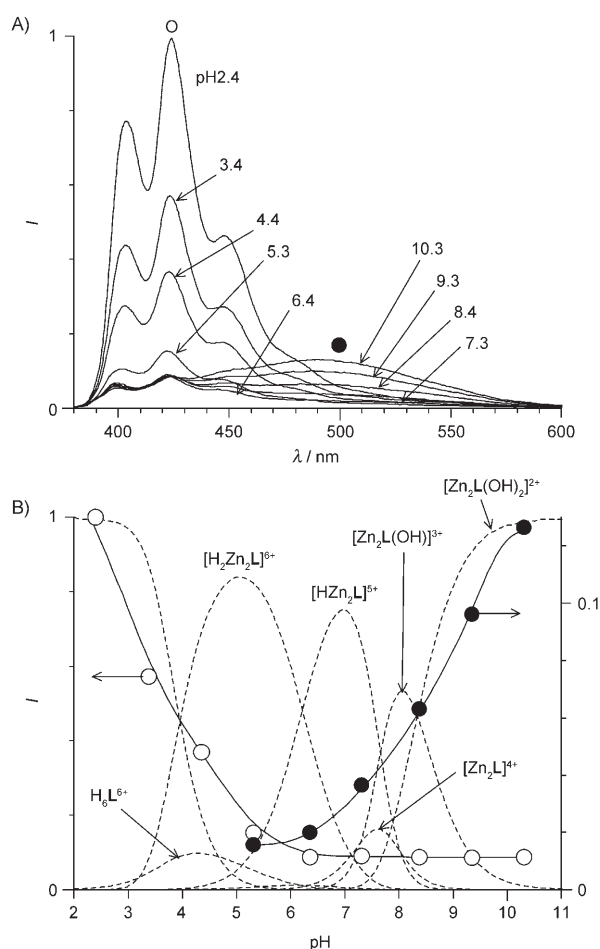


Figure 3. A) pH-dependent change in fluorescence spectra ($\lambda_{ex} = 368$ nm; 298 K) of **L** (50 μM) in aqueous NaClO$_4$ (0.15 M) solution with Zn$^{2+}$ (2 equiv). B) pH-dependent change in $I_M$ (monitored at 420 nm, ○), $I_E$ (monitored at 500 nm, ●), and mole fraction distribution of the different **L** species (-----), in which H$_8$L$^{8+}$ and H$_7$L$^{7+}$ species are shown as their total quantities. Each spectrum in A) corresponds to the plots in B).

Beer's Law plot (concentration of **L**+2Zn$^{2+}$ versus the absorbance at 450 nm) gives a straight line over the entire pH range. These findings indicate that the absorption rise at > 400 nm (Figure 4A) is due to neither intermolecular aggregation of **L** nor precipitation of **L** in solution. As reported for several ligand-conjugated aromatics,[16] coordination of metal cations with the ligand leads to formation of a metal–aromatic moiety π complex via donation of a π electron of the aromatic moiety to the adjacent metal cation at room temperature. The rising absorption of **L** at > 400 nm (Figure 4A) may therefore be due to the formation of a Zn$^{2+}$–AN π complex. A similar increase in absorption is observed for some ligand-conjugated AN molecules through Zn$^{2+}$–AN π complex formation.[17] As shown in Figure 3B, almost no $I_E$ increase is observed at pH 4–7. This is likely to be because the Zn$^{2+}$–AN π complex suppresses the photoexcitation of the AN fragments.[18] However, as shown in Figure 4A, the absorption of **L** decreases at pH > 7, at which OH$^-$-coordinated [Zn$_2$L(OH)]$^{3+}$ and [Zn$_2$L(OH)$_2$]$^{2+}$ species form (Figure 3B). This is because OH$^-$ coordination to the

Table 2. Logarithms of the stability constants for complexation between **L** and one or two equivalents of metal cations determined in aqueous NaClO$_4$ (0.15 M) solution at 298 K.

| Reaction[a] | Zn$^{2+}$ (2 equiv) | Cd$^{2+}$ (2 equiv) |
|---|---|---|
| 2H+2M+L→H$_2$M$_2$L | 37.80±0.98 | 35.20±0.09 |
| H+2M+L→HM$_2$L | 31.63±0.44 | 28.63±0.09 |
| 2M+L→M$_2$L | 23.40±2.38 | 19.90±0.13 |
| 2M+L+OH→M$_2$L(OH) | 30.10±2.38 | 24.90±0.13 |
| 2M+L+2OH→M$_2$L(OH)$_2$ | 35.40±2.38 | 29.60±0.13 |
| H+H$_2$M$_2$L→H$_3$M$_2$L | | 5.4 |
| H+HM$_2$L→H$_2$M$_2$L | 6.2 | 6.6 |
| H+M$_2$L→HM$_2$L | 8.2 | 8.7 |
| M$_2$L+OH→M$_2$L(OH) | 6.7 | 5.0 |
| M$_2$L(OH)+OH→M$_2$L(OH)$_2$ | 5.3 | 4.7 |
| M+ML→M$_2$L | 8.1 | 7.0 |

| | Zn$^{2+}$ (1 equiv) | Cd$^{2+}$ (1 equiv) |
|---|---|---|
| 4H+M+L→H$_4$ML | | 42.72±0.08 |
| 3H+M+L→H$_3$ML | 38.33±0.24 | 36.63±0.11 |
| 2H+M+L→H$_2$ML | 31.84±0.21 | 30.65±0.07 |
| H+M+L→HML | 24.49±0.21 | 22.83±0.08 |
| M+L→ML | 15.33±0.38 | 12.89±0.55 |
| M+L+OH→ML(OH) | 20.13±0.38 | 18.29±0.55 |
| 3H+2M+L→H$_3$M$_2$L | | 40.56±0.15 |
| H+H$_3$ML→H$_4$ML | | 6.1 |
| H+H$_2$ML→H$_3$ML | 6.5 | 6.0 |
| H+HML→H$_2$ML | 7.4 | 7.8 |
| H+ML→HML | 9.2 | 9.9 |
| ML+OH→ML(OH) | 4.8 | 5.4 |

[a] Charges are omitted for clarity.

Zn$^{2+}$ centers within **L** leads to a decrease in electronegativity of Zn$^{2+}$ and, hence, suppresses the formation of the Zn$^{2+}$–AN π complex,[18,19] thus probably allowing the appearance of the excimer emission at pH > 7 (Figure 3A).

Figure 4B shows the pH-dependent change in the excitation spectra of **L** collected at 420 nm (monomer emission) with two equivalents of Zn$^{2+}$. The spectra are similar to that obtained without metal cations (Figure 2B). In contrast, as shown in Figure 4C, excitation spectra collected at 500 nm (excimer emission) show a red-shifted band (400–440 nm) at pH > 7, at which OH$^-$-coordinated [Zn$_2$L(OH)]$^{3+}$ and [Zn$_2$L(OH)$_2$]$^{2+}$ species exist (Figure 3B). This band increases with increasing pH, which is consistent with the increase in $I_E$ (Figure 3B). This result implies that the excimer emission of **L** is due to a "static" excimer formed by direct photoexcitation of the intramolecular GSD[17a,18a,20] of the bipolar AN fragments within **L**.

Figure 5 shows decay profiles of the monomer and excimer emissions of **L** ($\lambda_{ex}$ = 370 nm) measured with two equivalents of Zn$^{2+}$ at pH 10.3, at which [Zn$_2$L(OH)$_2$]$^{2+}$ exists. Table 3 summarizes the decay times and preexponential factors of the emitting components. Both profiles are successfully fitted by the sums of two exponentials with short and long lifetimes, for which no negative preexponential, that is, a rise time, is detected. The respective emitting components are assigned to the monomer (8.3 ns) and excimer (38.6 ns) species. These findings clearly indicate that the excimer emission of **L** is due to the "static" excimer formed by direct photoexcitation of the GSD formed between the bipolar AN fragments. The lack of a red-shifted GSD excita-
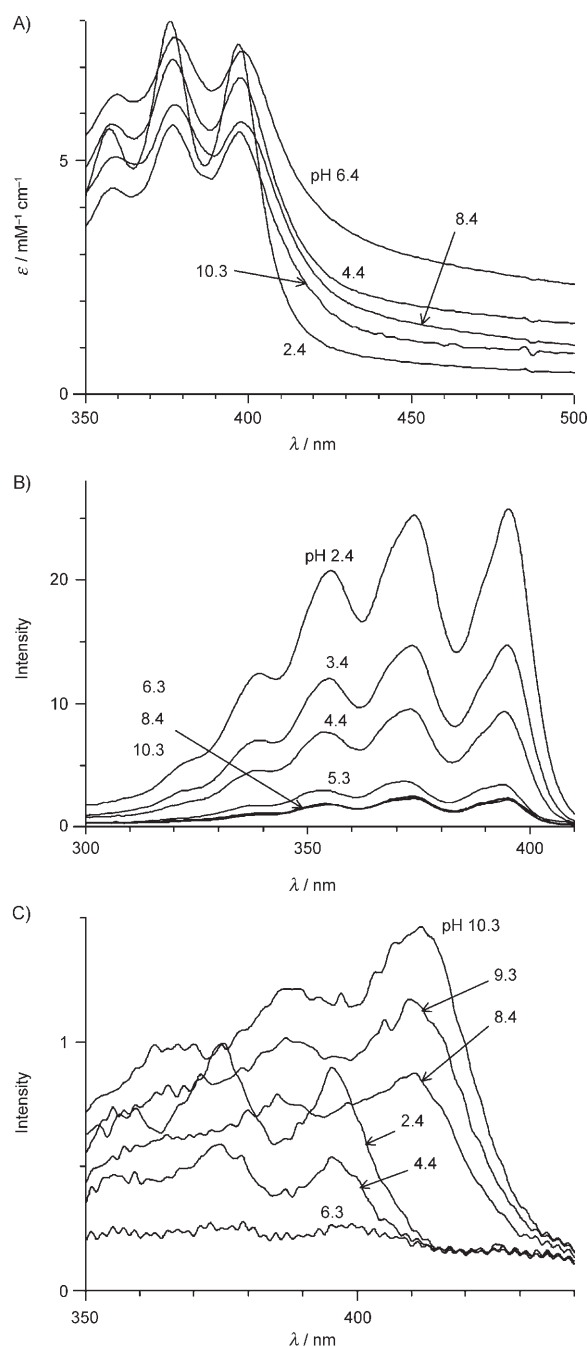


Figure 4. pH-dependent change in A) absorption spectra and excitation spectra collected at B) 420 nm (monomer emission) and C) 500 nm (excimer emission) of **L** with Zn$^{2+}$ (2 equiv) in aqueous NaClO$_4$ (0.15 M) solution at 298 K.

tion band at pH 4–7 (Figure 4C) is because the Zn$^{2+}$–AN π complex suppresses the π-stacking interaction of the bipolar AN fragments, resulting in suppression of GSD formation. The appearance of the red-shifted GSD excitation band at pH > 7 (Figure 4C) is because the OH$^-$ coordination to the Zn$^{2+}$ centers leads to a decrease in the electronegativity of Zn$^{2+}$ and, hence, suppresses the formation of the Zn$^{2+}$–AN π complex. This allows π-stacking interactions of
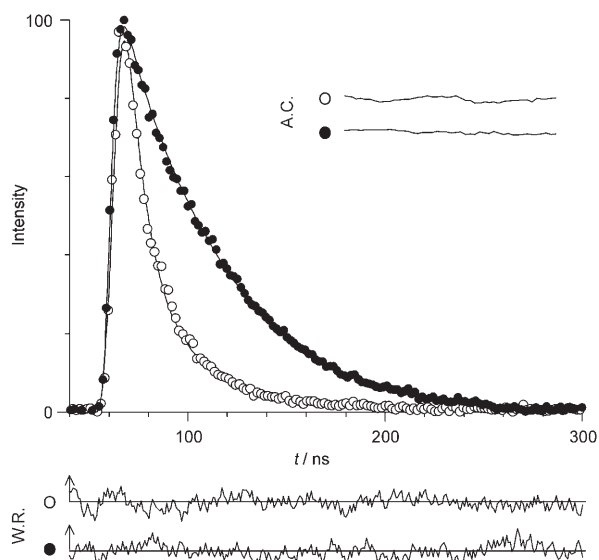
Figure 5. Decay profiles ($\lambda_{ex} = 370$ nm; 298 K) of monomer emission (monitored at 420 nm, ○) and excimer emission (monitored at 500 nm, ●) of **L** measured with $Zn^{2+}$ (2 equiv) in aqueous $NaClO_4$ (0.15 M) solution at pH 10.3. For judging the quality of the fit, autocorrelation functions (A.C.) and weighted residuals (W.R.) are also shown.

Table 3. Decay times ($\tau$) and preexponential factors ($a$) of monomer and excimer components for emissions of the respective **L** complexes at pH 10.3 ($\lambda_{ex} = 370$ nm).

| Species | $\lambda_{em}$ [nm] | $\tau_{monomer}$ [ns] ($a_{monomer}$ [%]) | $\tau_{excimer}$ [ns] ($a_{excimer}$ [%]) | $\chi^2$ |
|---|---|---|---|---|
| $[ZnL(OH)]^+$ | 420 | 8.4 (97.5) | 39.0 (2.5) | 2.19 |
| | 500 | 8.4 (46.5) | 39.0 (53.5) | 3.12 |
| $[Zn_2L(OH)_2]^{2+}$ | 420 | 8.3 (98.4) | 38.6 (1.6) | 2.05 |
| | 500 | 8.3 (43.4) | 38.6 (56.6) | 1.94 |
| $[ZnCdL(OH)_2]^{2+}$ ($Zn^{2+} \rightarrow Cd^{2+}$ sequence) | 420 | 8.0 (97.3) | 37.1 (2.7) | 2.69 |
| | 500 | 8.0 (70.5) | 37.1 (29.5) | 2.00 |
| $[CdL(OH)]^+$ | 420 | 7.9 (100) | | 2.98 |
| $[Cd_2L(OH)_2]^{2+}$ | 420 | 8.1 (100) | | 2.09 |
| $[ZnCdL(OH)_2]^{2+}$ ($Cd^{2+} \rightarrow Zn^{2+}$ sequence) | 420 | 10.0 (100) | | 1.55 |

the bipolar AN fragments (GSD formation), resulting in an increase in $I_E$ at pH > 7 (Figure 3B).

Figure 6A shows the emission spectra of **L** obtained with one equivalent of $Zn^{2+}$. As is also the case with two equivalents of $Zn^{2+}$ (Figure 3A), excimer emission appears at basic pH values. As shown in Figure 6B, $I_E$ increases dramatically at pH > 8, along with the formation of $OH^-$-coordinated $[ZnL(OH)]^+$ species. As shown in Figure 6C, the absorbance of **L** at > 400 nm rises with increasing pH in the range of 5–8, at which $OH^-$-free $Zn^{2+}$–**L** complexes ($[ZnH_3L]^{5+}$, $[ZnH_2L]^{4+}$, and $[ZnHL]^{3+}$) exist. This increased absorption, however, drops at pH > 8, at which the $OH^-$-coordinated $[ZnL(OH)]^+$ species forms. This is because $OH^-$ coordination to the $Zn^{2+}$ center suppresses the formation of the $Zn^{2+}$–AN $\pi$ complex, as is also the case with two equivalents of $Zn^{2+}$.
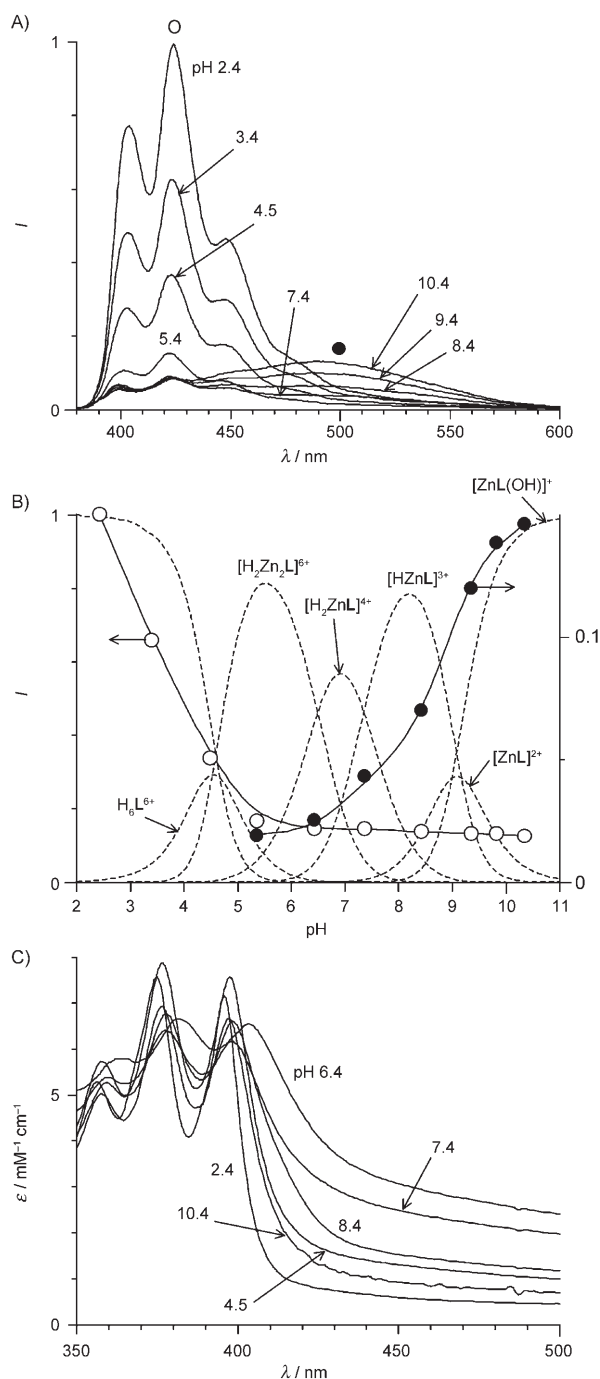


Figure 6. A) pH-dependent change in fluorescence spectra ($\lambda_{ex} = 368$ nm; 298 K) of **L** (50 μM) in aqueous $NaClO_4$ (0.15 M) solution with $Zn^{2+}$ (1 equiv). B) pH-dependent change in $I_M$ (monitored at 420 nm, ○), $I_E$ (monitored at 500 nm, ●), and mole fraction distribution of different **L** species (-----), in which $H_8L^{8+}$ and $H_7L^{7+}$ species are shown as their total quantities. C) pH-dependent change in absorption spectra.

Figure 7A shows the change in the emission spectra of **L** with stepwise $Zn^{2+}$ addition at pH 10.3. Changes in $I_M$ and $I_E$ are summarized in Figure 7B. Addition of $Zn^{2+}$ leads to an increase in $I_M$, but the increase is saturated upon addition of one equivalent of $Zn^{2+}$. At pH 10.3 with one equivalent of $Zn^{2+}$ (Figure 6B), $[ZnL(OH)]^+$ exists, in which one poly-
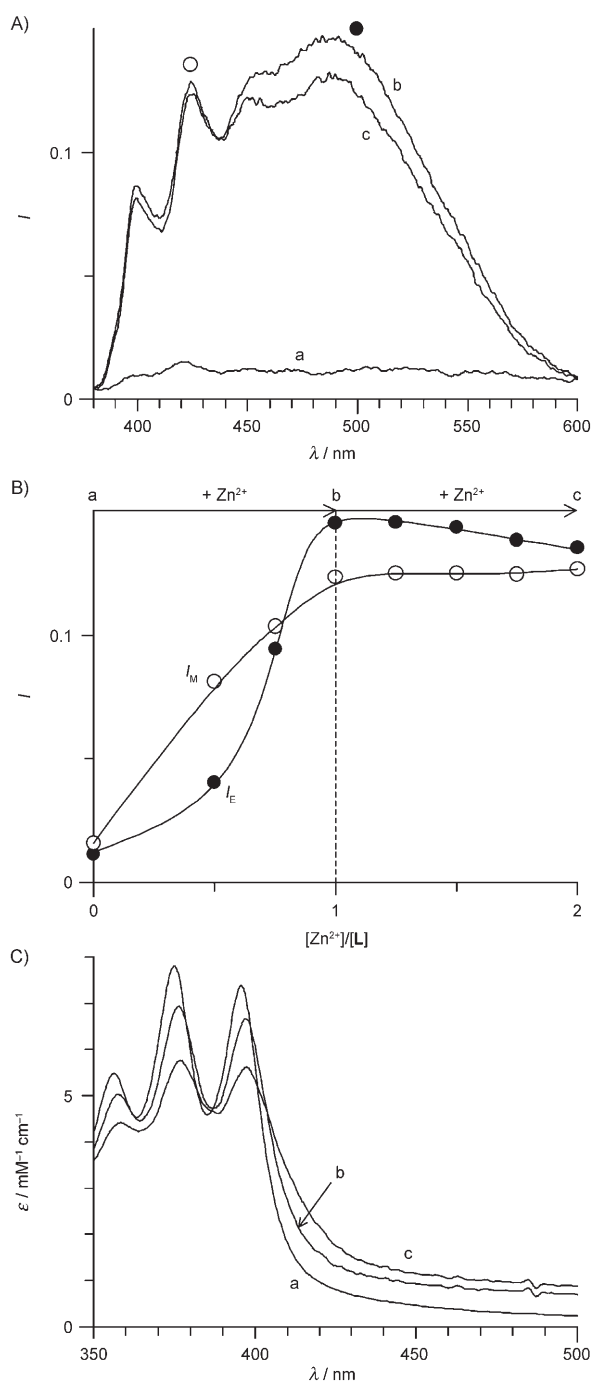
A)



B)

C)

Figure 7. Changes in A) fluorescence spectra, B) $I_M$ and $I_E$, and C) absorption spectra of **L** at pH 10.3 (298 K) with amount of $Zn^{2+}$: a) zero, b) 1 equiv, c) 2 equiv.
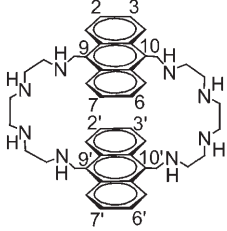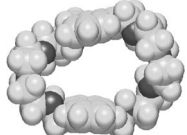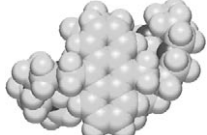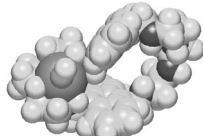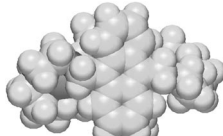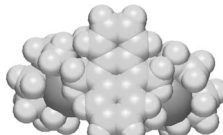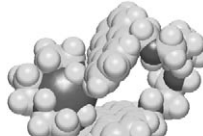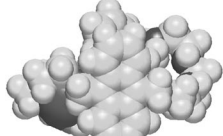
amine bridge of **L** coordinates with $Zn^{2+}$ and the other has four deprotonated and metal-free nitrogen atoms. In contrast, with two equivalents of $Zn^{2+}$ at pH 10.3 (Figure 3B), $[Zn_2\mathbf{L}(OH)_2]^{2+}$ exists, in which each of the bridges of **L** coordinates with one $Zn^{2+}$ center. The saturation of the increase in $I_M$ upon addition of one equivalent of $Zn^{2+}$ (Figure 7B) means that $[Zn_2\mathbf{L}(OH)_2]^{2+}$ shows an $I_M$ value simi-

lar to that of $[Zn\mathbf{L}(OH)]^+$, although ET from the nitrogen atoms to the excited AN monomer might be much suppressed within $[Zn_2\mathbf{L}(OH)_2]^{2+}$ because all nitrogen atoms coordinate with $Zn^{2+}$. The lack of a gain in $I_M$ upon coordination of two $Zn^{2+}$ centers is due to the weak coordination of the second $Zn^{2+}$, which leads to ET from nitrogen atoms to the excit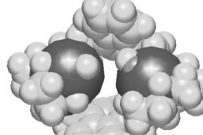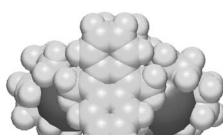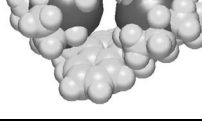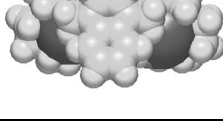ed AN monomer. The first $Zn^{2+}$ coordination with one polyamine bridge of **L** leads to a distortion of the other bridge; therefore, the second $Zn^{2+}$ coordination is structurally restricted, resulting in weak coordination. In particular, as reported,[21] benzylic nitrogen atoms of the bridges are coplanar and close to the AN fragment, which may mainly contribute to the weak coordination with the second $Zn^{2+}$ center. As shown in Table 2, the stability constant for coordination of **L** with a second $Zn^{2+}$ center ($Zn^{2+}$ $+[Zn\mathbf{L}]^{2+}\rightarrow[Zn_2\mathbf{L}]^{4+}$; $\log K_a = 8.1$) is lower than that of the first $Zn^{2+}$ center ($Zn^{2+}+\mathbf{L}\rightarrow[Zn\mathbf{L}]^{2+}$; $\log K_a = 15.3$); this finding supports the weak coordination with the second $Zn^{2+}$ center. These results indicate that the weak coordination of the second $Zn^{2+}$ center still leads to ET to the excited AN monomer, resulting in almost no gain of $I_M$ by the second $Zn^{2+}$ coordination (Figure 7B). As shown in Table 3, the lifetime of the monomer component of $[Zn_2\mathbf{L}(OH)_2]^{2+}$ (8.3 ns) is almost the same as that of $[Zn\mathbf{L}(OH)]^+$ (8.4 ns).

As shown in Figure 7B, $I_E$ also increases with $Zn^{2+}$ addition; however, the addition of two equivalents of $Zn^{2+}$ leads to a 10% lower $I_E$ than that obtained with one equivalent of $Zn^{2+}$. This finding is explained by the distance between the bipolar AN fragments within **L**. Table 4 summarizes the distances within $[Zn\mathbf{L}(OH)]^+$ and $[Zn_2\mathbf{L}(OH)_2]^{2+}$ complexes determined by semiempirical molecular orbital (MO) calculations. The average distance between the bipolar AN fragments is 6.64 Å ($[Zn\mathbf{L}(OH)]^+$) and 7.44 Å ($[Zn_2\mathbf{L}(OH)_2]^{2+}$), which means that the second $Zn^{2+}$ coordination brings the AN fragments apart. As a result of this, the π-stacking interaction of the AN fragments becomes weaker (GSD stability decrease), thus leading to a decrease in $I_E$ upon the second $Zn^{2+}$ coordination (Figure 7B). As shown in Table 3, the lifetime of the excimer component of $[Zn_2\mathbf{L}(OH)_2]^{2+}$ is shorter than that of $[Zn\mathbf{L}(OH)]^+$, which means that the GSD is actually destabilized by the second $Zn^{2+}$ coordination.

**Effect of $Cd^{2+}$ addition**: Figures 8A and 9A show the pH-dependent change in the emission spectra of **L** obtained with two and one equivalents of $Cd^{2+}$, respectively. As summarized in Figures 8B and 9B, $I_M$ decreases with pH increase but is constant at pH > 6 (at 90% decreased level), with pH–$I_M$ profiles similar to those obtained with $Zn^{2+}$ (Figures 3B and 6B, open symbols). The appearance of monomer emission even at basic pH values is because $Cd^{2+}$ coordination with a polyamine bridge suppresses ET from the nitrogen atoms to the excited AN fragment,[18] as is also the case with $Zn^{2+}$. A notable feature of the emission spectra of **L** obtained with $Cd^{2+}$ is that excimer emission does not appear at any pH. At pH > 8 with two and one equivalents of $Cd^{2+}$, $OH^-$-coordinated $[Cd\mathbf{L}(OH)]^+$ and $[Cd_2\mathbf{L}(OH)_2]^{2+}$

Table 4. Distance between the bipolar AN fragments within **L** determined by semiempirical MO calculations.

| | | | Distance [Å] |
|---|---|---|---|
| | | | 2–2' |
| | | | 3–3' |
| | | | 7–7' |
| | | | 6–6' |
| | | | 9–9' |
| | | | 10–10' |
| | | | (average) |
| Complex | Side view | Top view | |
| **L** | | | 7.74 |
| | | | 7.90 |
| | | | 8.59 |
| | | | 8.70 |
| | | | 8.32 |
| | | | 8.63 |
| | | | (8.31) |
| [Zn**L**(OH)]$^+$ | | | 5.31 |
| | | | 6.34 |
| | | | 7.36 |
| | | | 8.06 |
| | | | 5.45 |
| | | | 7.33 |
| | | | (6.64) |
| [Zn$_2$**L**(OH)$_2$]$^{2+}$ | | | 4.76 |
| | | | 4.49 |
| | | | 11.13 |
| | | | 11.19 |
| | | | 6.65 |
| | | | 6.40 |
| | | | (7.44) |
| [Cd**L**(OH)]$^+$ | | | 8.34 |
| | | | 9.02 |
| | | | 5.89 |
| | | | 6.69 |
| | | | 6.05 |
| | | | 7.75 |
| | | | (7.29) |
| [Cd$_2$**L**(OH)$_2$]$^{2+}$ | | | 5.65 |
| | | | 5.71 |
| | | | 11.09 |
| | | | 11.10 |
| | | | 6.96 |
| | | | 7.06 |
| | | | (7.93) |

species form predominantly, as is also the case with Zn$^{2+}$; however, no excimer emission appears.

Figures 8C and 9C show the pH-dependent change in the absorption spectra of **L** obtained with Cd$^{2+}$. The absorbance of **L** "rises" with increase in pH, as is also the case with Zn$^{2+}$ (Figures 4A and 6A). However, the absorbance "red-shifts" (about 4 nm) with a pH increase (see around 400 nm), which is associated with the coordination of Cd$^{2+}$ (Figures 8B and 9B). The increased and red-shifted absorption of **L** may be due to the formation of a Cd$^{2+}$–AN π complex through donation of a π electron of the AN fragments to the adjacent Cd$^{2+}$ center.[18b] Notably, the absorp-

tion of **L** does not decrease even at basic pH, although the addition of Zn$^{2+}$ leads to a clear decrease (Figures 4A and 6C). Figure 10B shows the $^1$H NMR spectra of **L** measured with or without Cd$^{2+}$ in D$_2$O/CD$_3$CN (8:2, v/v) at pH 10.3. With one and two equivalents of Cd$^{2+}$ (where [Cd**L**(OH)]$^+$ and [Cd$_2$**L**(OH)$_2$]$^{2+}$ exist), **L** shows a downfield shift of AN resonance, which is assigned to formation of the Cd$^{2+}$–AN π complex.[14a] In contrast, as shown in Figure 10A, addition of Zn$^{2+}$ does not show a downfield shift. This finding suggests that, as reported for ligand-conjugated AN molecules,[17,18] the Cd$^{2+}$–AN π complex is stronger than the Zn$^{2+}$–AN π complex. The appearance of the increased and red-shifted absorption of **L** with Cd$^{2+}$ even at basic pH (Figures 8C and 9C) suggests that the Cd$^{2+}$–AN π complex is much stronger and is not relieved by OH$^-$ coordination to the Cd$^{2+}$ centers. The formation of the strong Cd$^{2+}$–AN π complex suppresses the π-stacking interaction of the bipolar AN fragments and, hence, suppresses formation of the GSD, resulting in no excimer emission (Figures 8A and 9A). These results indicate that **L** behaves as a fluorescent molecular switch capable of showing Zn$^{2+}$-selective excimer emission. So far, this type of emission has been achieved by two molecules;[22] however, these systems employ a pyrene or naphthalene fluorophore. The present **L** system is the first example showing Zn$^{2+}$-selective AN excimer emission.

Figure 11A shows the change in the emission spectra of **L** with stepwise Cd$^{2+}$ addition at pH 10.3. No excimer emission appears because of the formation of the Cd$^{2+}$–AN π complex: the increased and red-shifted absorption appears after addition of the entire amount of Cd$^{2+}$ (Figure 11C). In contrast, as shown in Figure 11B, $I_M$ increases with increasing amount of Cd$^{2+}$ but is saturated upon addition of one equivalent of Cd$^{2+}$, as is also the case for Zn$^{2+}$ (Figure 7B). At pH 10.3 with one and two equivalents of Cd$^{2+}$,
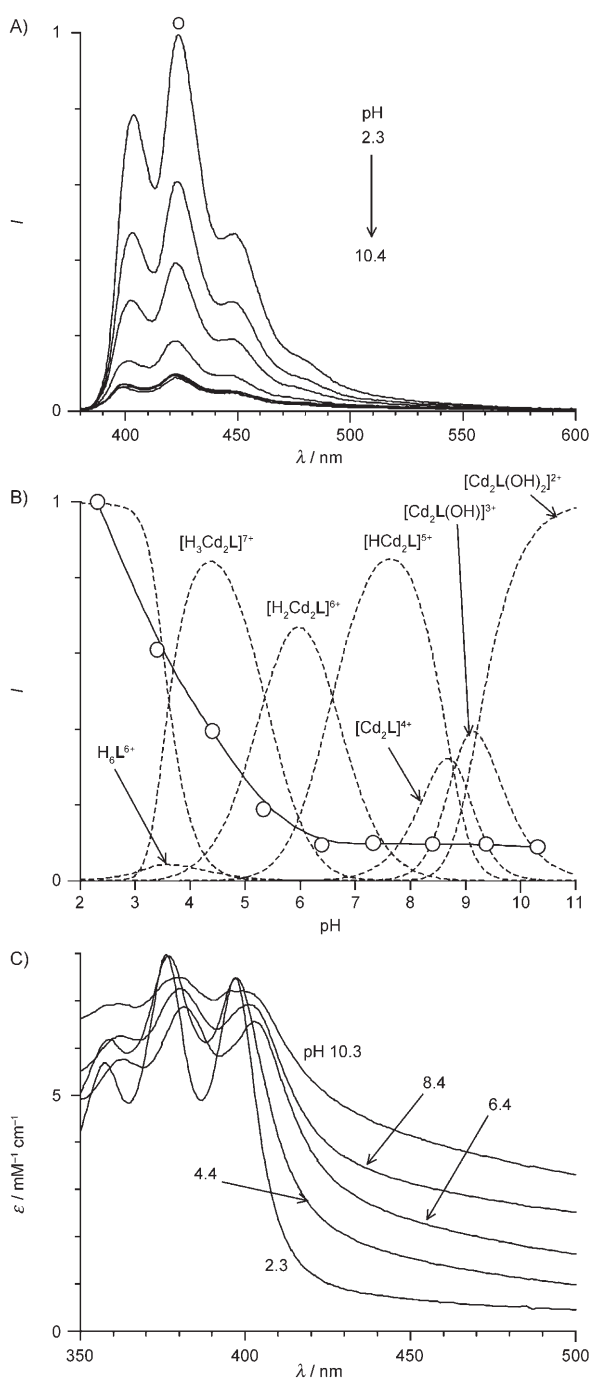
Figure 8. A) pH-dependent change in fluorescence spectra ($\lambda_{ex} = 368$ nm; 298 K) of **L** (50 μM) in aqueous NaClO$_4$ (0.15 M) solution with Cd$^{2+}$ (2 equiv). B) pH-dependent change in $I_M$ (monitored at 420 nm) and mole fraction distribution of the species (-----), in which H$_8$**L**$^{8+}$ and H$_7$**L**$^{7+}$ are shown as their total quantities. C) pH-dependent change in absorption spectra. Each spectrum in A) corresponds to the plots in B).
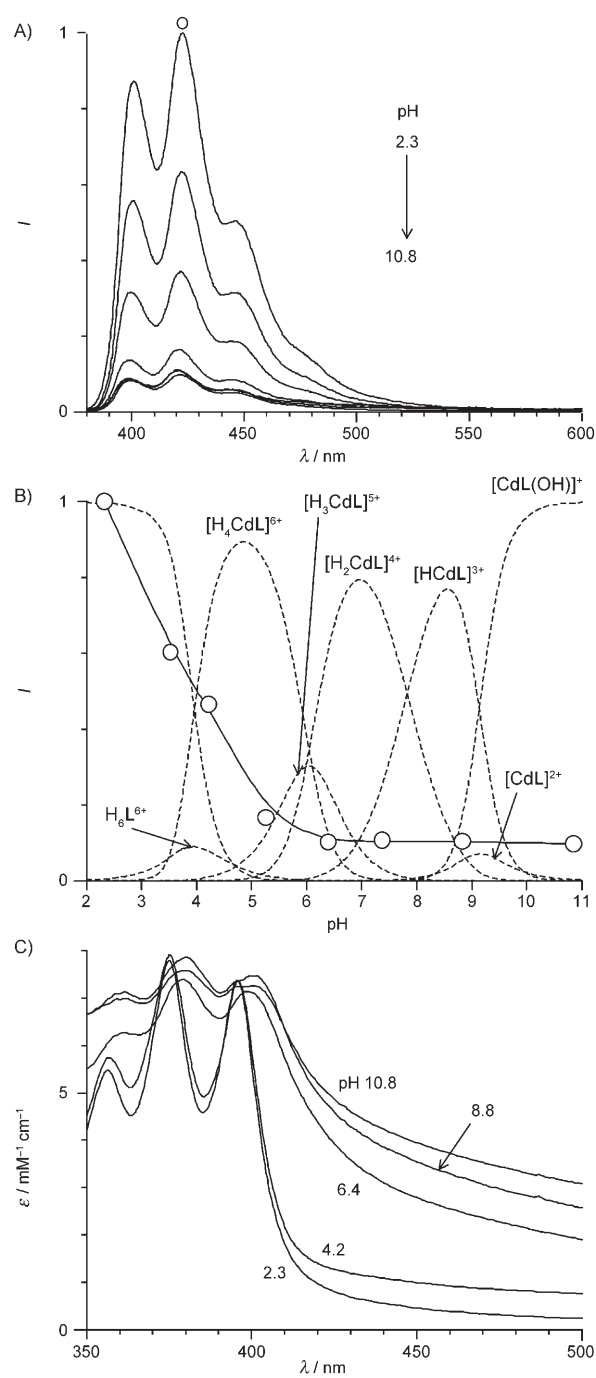
Figure 9. A) pH-dependent change in fluorescence spectra ($\lambda_{ex} = 368$ nm; 298 K) of **L** (50 μM) in aqueous NaClO$_4$ (0.15 M) solution with Cd$^{2+}$ (1 equiv). B) pH-dependent change in $I_M$ (monitored at 420 nm) and mole fraction distribution of the species (-----), in which H$_8$**L**$^{8+}$ and H$_7$**L**$^{7+}$ are shown as their total quantities. C) pH-dependent change in absorption spectra. Each spectrum in A) corresponds to the plots in B).

[CdL(OH)]$^+$ and [Cd$_2$L(OH)$_2$]$^{2+}$ exist (Figures 8B and 9B). In the [CdL(OH)]$^+$ complex, one polyamine bridge of **L** coordinates with the Cd$^{2+}$ center and the other has four deprotonated and metal-free nitrogen atoms. In contrast, in the [Cd$_2$L(OH)$_2$]$^{2+}$ complex, all nitrogen atoms coordinate with Cd$^{2+}$. The lack of a gain in $I_M$ even upon coordination

of two Cd$^{2+}$ centers (Figure 11B) is due to the weak coordination of the second Cd$^{2+}$ center with a polyamine bridge, as is also the case with Zn$^{2+}$: the first Cd$^{2+}$ coordination with one bridge of **L** leads to distortion of the other bridge and, hence, leads to weak coordination of the second Cd$^{2+}$ center. This leads to ET from the nitrogen atoms to the ex-
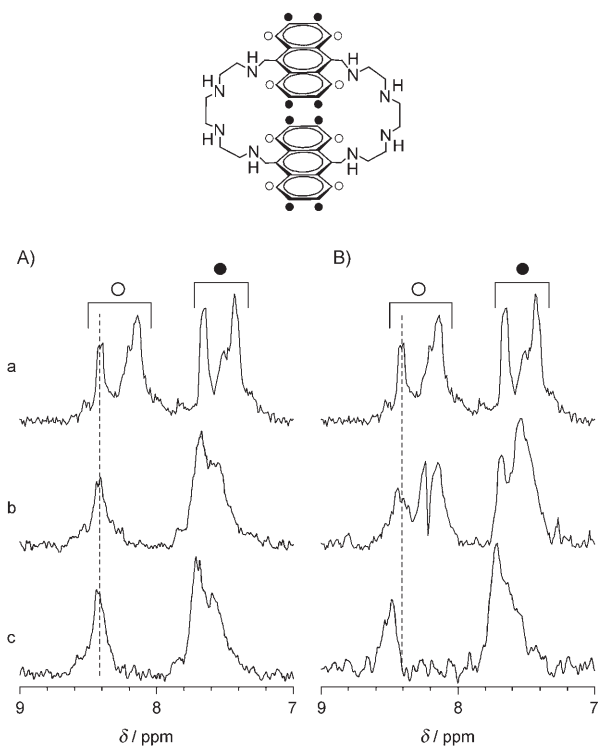
Figure 10. $^1$H NMR spectra of **L** in $D_2O/CD_3CN$ (80:20, v/v; pH 10.3) solution measured a) without metal cations and with b) 1 equiv and c) 2 equiv of A) $Zn^{2+}$ and B) $Cd^{2+}$. pH ($=pD-0.4$) of the solution was adjusted with DCl and NaOD.
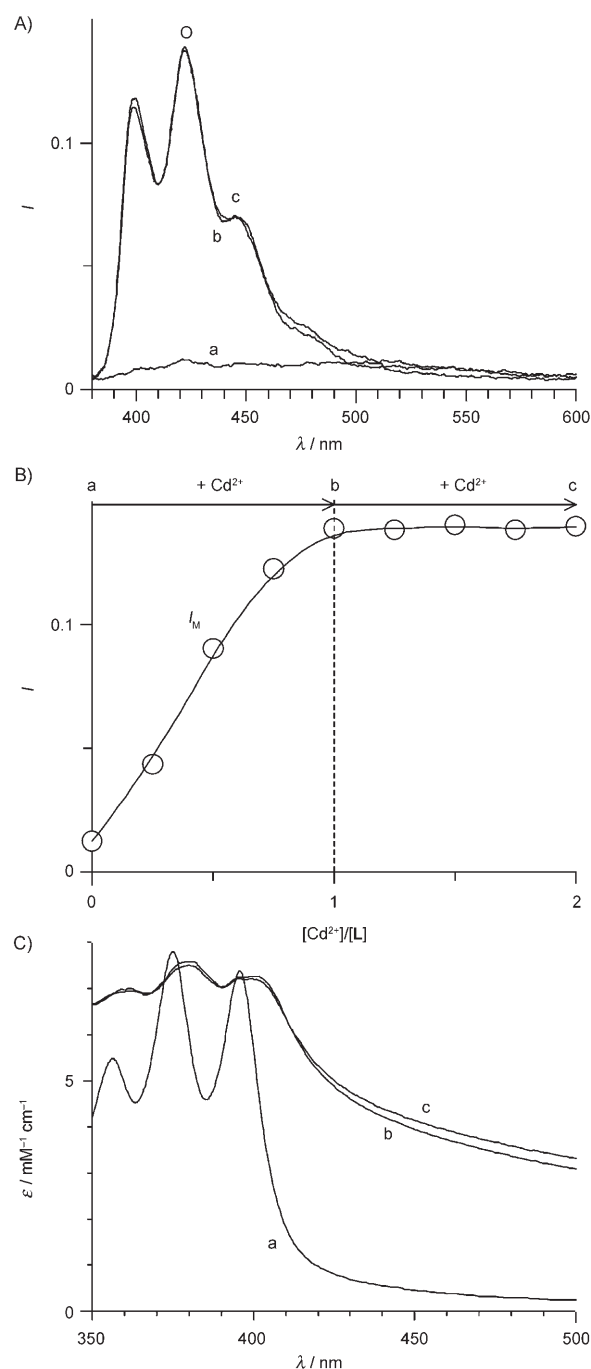


Figure 11. Change in A) fluorescence spectra, B) $I_M$, and C) absorption spectra of **L** at pH 10.3 (298 K) with amount of $Cd^{2+}$: a) zero, b) 1 equiv, c) 2 equiv.

cited AN, resulting in almost no $I_M$ gain upon coordination of the second $Cd^{2+}$ center. As shown in Table 2, the stability constant for coordination of the second $Cd^{2+}$ center ($Cd^{2+}+$ $[CdL]^{2+}\rightarrow[Cd_2L]^{4+}$; $\log K_a=7.0$) is lower than that of the first $Cd^{2+}$ center ($Cd^{2+}+L\rightarrow[CdL]^{2+}$; $\log K_a=12.9$). This result supports the weak coordination of the second $Cd^{2+}$ center. Table 3 summarizes the lifetimes of monomer emission for the $[CdL(OH)]^+$ and $[Cd_2L(OH)_2]^{2+}$ complexes. The lifetimes of both complexes (7.9 and 8.1 ns) are relatively shorter than that for $[ZnL(OH)]^+$ and $[Zn_2L(OH)_2]^{2+}$ complexes (8.4 and 8.3 ns). This may be because the stronger $Cd^{2+}$–AN $\pi$ complex quenches the excited AN monomer more significantly.[17,18]

**Effect of input sequence of metal cations**: The most notable feature of **L** is the irreversible switching of excimer emission driven by the input sequence of metal cations. Figure 12A shows the change in the emission spectra of **L** upon sequential addition of $Zn^{2+}$ and $Cd^{2+}$ (each one equivalent) at pH 10.3 ($Zn^{2+}\rightarrow Cd^{2+}$ sequence). As shown in Figure 12B, $I_M$ remains constant even upon addition of $Cd^{2+}$ to a solution containing one equivalent of $Zn^{2+}$, as is also the case for the $Zn^{2+}\rightarrow Zn^{2+}$ sequence (Figure 7B). In this case, $I_E$ decreases with the addition of $Cd^{2+}$ due to the formation of the $Cd^{2+}$–AN $\pi$ complex, but still appears at a 50% decreased level.

Figure 13A shows the change in the emission spectra of **L** upon sequential addition of $Cd^{2+}$ and $Zn^{2+}$ (each one equiv-

alent) at pH 10.3 ($Cd^{2+}\rightarrow Zn^{2+}$ sequence). As shown in Figure 13B, upon addition of one equivalent of $Zn^{2+}$ to a solution containing one equivalent of $Cd^{2+}$, $I_M$ remains constant, but excimer emission does not appear. These findings indicate that the $Zn^{2+}\rightarrow Cd^{2+}$ sequence allows the appearance of both monomer and excimer emission, whereas the reverse sequence allows only monomer emission. As shown in Figure 12C, in the $Zn^{2+}\rightarrow Cd^{2+}$ sequence, $Cd^{2+}$ addition scarcely shows red-shifted absorption. In contrast, for the re-

Figure 12. Change in A) fluorescence spectra, B) $I_M$ and $I_E$, and C) absorption spectra of **L** at pH 10.3 (298 K) with the addition of cations in the sequence $Zn^{2+} \rightarrow Cd^{2+}$ (each 1 equiv): a) zero; b) 1 equiv of $Zn^{2+}$; c) 1 equiv of $Cd^{2+}$.
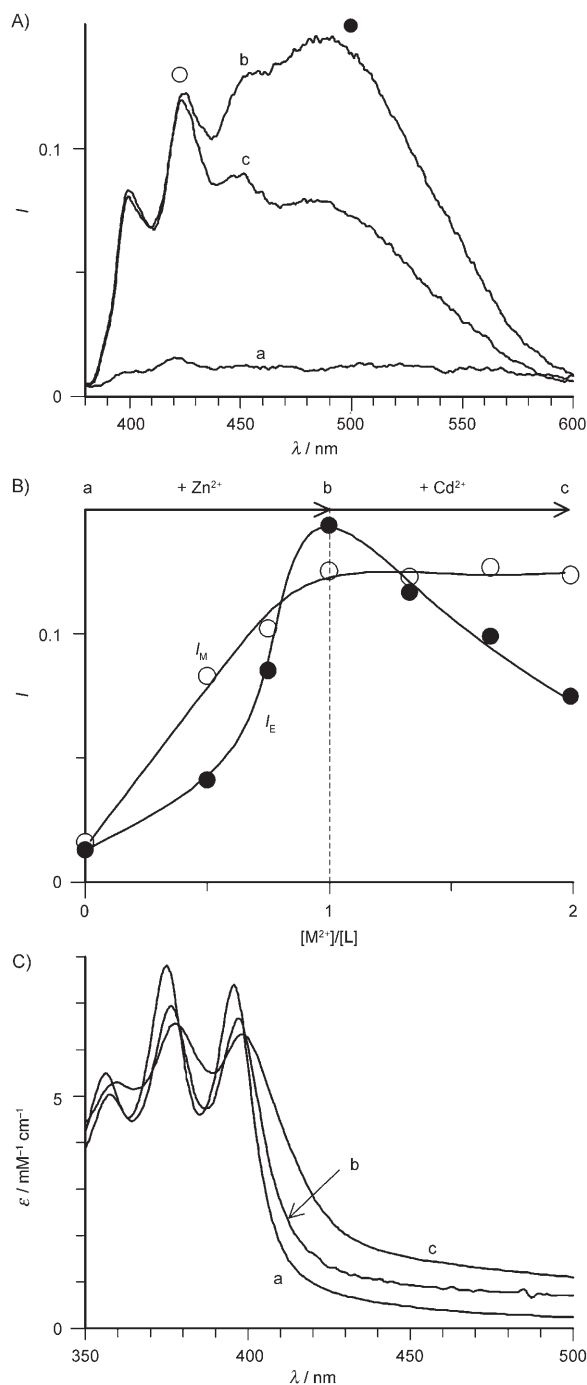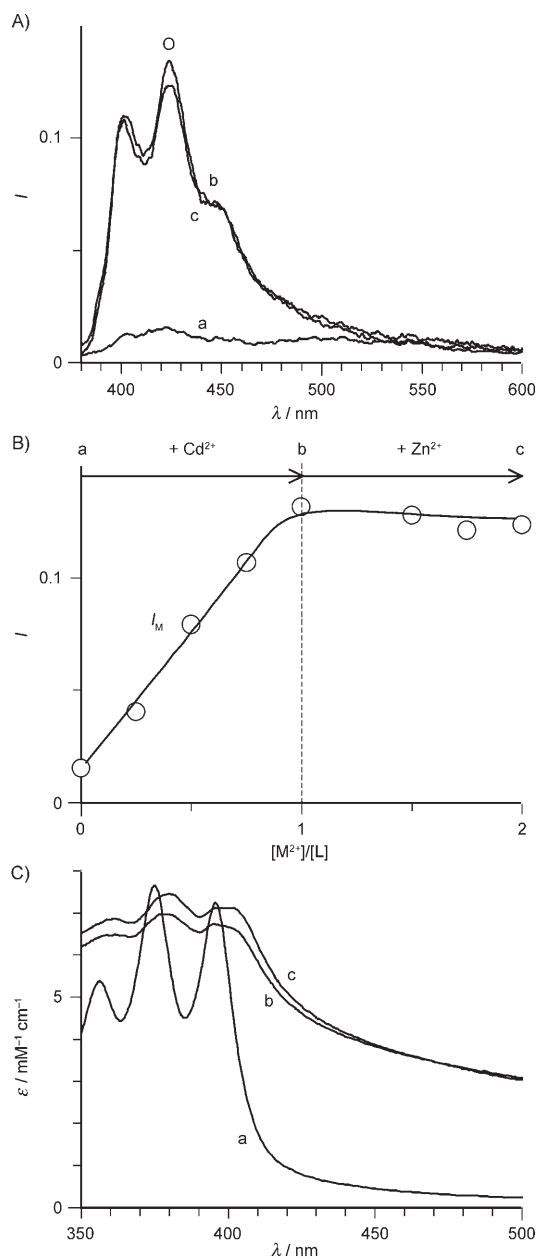


Figure 13. Change in A) fluorescence spectra, B) $I_M$, and C) absorption spectra of **L** at pH 10.3 (298 K) with the addition of cations in the sequence $Cd^{2+} \rightarrow Zn^{2+}$ (each 1 equiv): a) zero; b) 1 equiv of $Cd^{2+}$; c) 1 equiv of $Zn^{2+}$.

verse sequence, red-shifted absorption still remains upon $Zn^{2+}$ addition (Figure 13C). As shown in Figures 3B, 6B, 8B, and 9B, the mole fraction distributions of the species obtained with one or two equivalents of $Zn^{2+}$ or $Cd^{2+}$ reveal that, at pH 10.3, all species contain $OH^-$-coordinated $Zn^{2+}$ or $Cd^{2+}$ centers ([$ZnL(OH)]^+$, [$Zn_2L(OH)_2]^{2+}$, [$CdL(OH)]^+$, and [$Cd_2L(OH)_2]^{2+}$). This suggests that, at pH 10.3, both

$Zn^{2+} \rightarrow Cd^{2+}$ and $Cd^{2+} \rightarrow Zn^{2+}$ sequences produce the [$ZnCdL(OH)_2]^{2+}$ complex, in which each of the $Zn^{2+}$ and $Cd^{2+}$ centers coordinates with $OH^-$. These results mean that the [$ZnCdL(OH)_2]^{2+}$ complex produced by the $Cd^{2+} \rightarrow Zn^{2+}$ sequence forms a $Cd^{2+}$–AN π complex stronger than the complex formed by the reverse sequence, despite the same chemical composition.

Figure 14A shows the change in the $^1H$ NMR spectra of **L** with sequential $Zn^{2+} \rightarrow Cd^{2+}$ addition. The spectra do not show a downfield shift of the AN resonance, as is also the case for the $Zn^{2+} \rightarrow Zn^{2+}$ sequence (Figure 10A). In contrast,
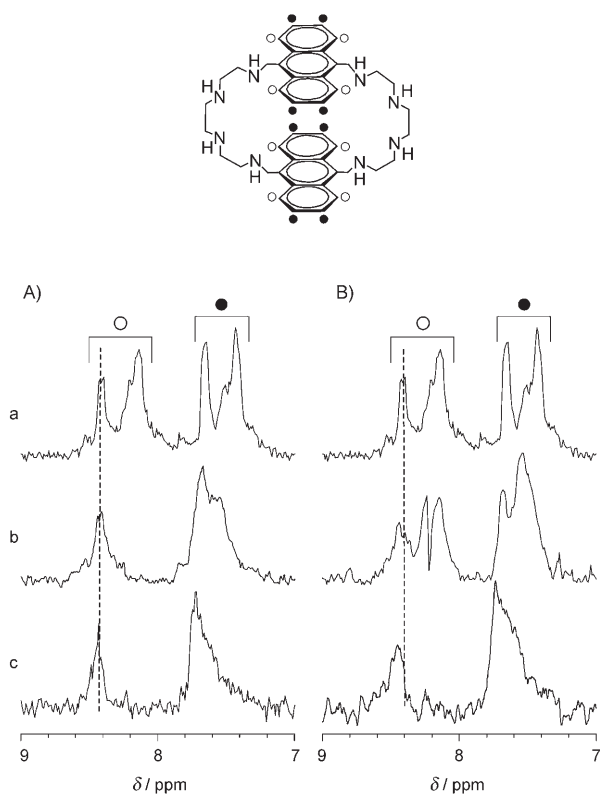
Figure 14. Change in $^1$H NMR spectra of **L** in $D_2O/CD_3CN$ (80:20, v/v; pH 10.3) with the addition of cations in the sequence A) $Zn^{2+} \rightarrow Cd^{2+}$ (a) zero, b) 1 equiv of $Zn^{2+}$, c) 1 equiv of $Cd^{2+}$) and B) $Cd^{2+} \rightarrow Zn^{2+}$ (a) zero, b) 1 equiv of $Cd^{2+}$, c) 1 equiv of $Zn^{2+}$). The pH (=pD−0.4) of the solution was adjusted with DCl and NaOD.



Figure 15. Change in A) fluorescence ($\lambda_{ex}=368$ nm; 298 K) and B) absorption spectra of **L** (50 μM) in aqueous $NaClO_4$ (0.15 M) solution at pH 10.3, when $Zn^{2+}$ and $Cd^{2+}$ were added at the same time: a) zero, b) 1 equiv each of $Zn^{2+}$ and $Cd^{2+}$.

for the $Cd^{2+} \rightarrow Zn^{2+}$ sequence (Figure 14B), the AN resonance shifted downfield by the first $Cd^{2+}$ coordination still remains upon sequential $Zn^{2+}$ coordination. This suggests that the first $Cd^{2+}$ coordination leads to formation of a strong $Cd^{2+}$–AN π complex. In contrast, for the $Zn^{2+} \rightarrow Cd^{2+}$ sequence, $Cd^{2+}$ coordination is structurally restricted by the first $Zn^{2+}$ coordination with the other polyamine bridge, thus probably leading to formation of a weak $Cd^{2+}$–AN π complex. As a result, the π-stacking interaction between the AN fragments is maintained even upon $Cd^{2+}$ coordination and, hence, leads to GSD formation, allowing the production of excimer emission. In contrast, for the $Cd^{2+} \rightarrow Zn^{2+}$ sequence, the first $Cd^{2+}$ coordination forms a stably configured strong $Cd^{2+}$–AN π complex whose configuration is maintained even upon sequential $Zn^{2+}$ coordination, resulting in no excimer emission (Figure 13A).

The mechanism for excimer emission switching by the input sequence of metal cations is confirmed experimentally. Figure 15A shows the change in the emission spectra of **L** upon addition of $Zn^{2+}$ (one equivalent) and $Cd^{2+}$ (one equivalent) at the same time. $I_M$ increases with the simultaneous addition of $Zn^{2+}$ and $Cd^{2+}$, but excimer emission does not appear. In this case, as shown in Figure 15B, an increased and red-shifted absorption appears, indicating that
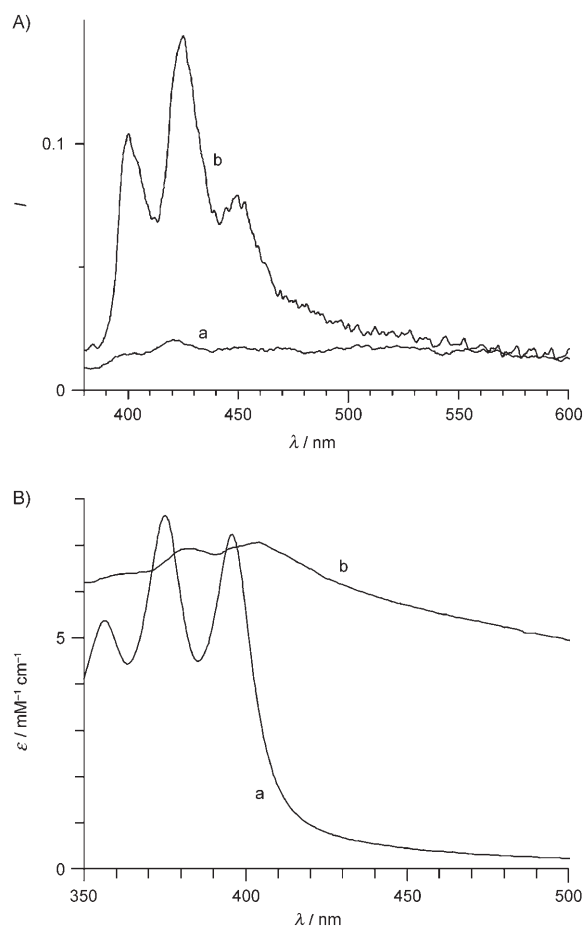
the simultaneous addition of $Zn^{2+}$ and $Cd^{2+}$ leads to the formation of a strong $Cd^{2+}$–AN π complex. This is because, as described,[23] $Cd^{2+}$ coordination with a polyamine ligand in water occurs more rapidly than $Zn^{2+}$ coordination. This result clearly suggests that the production of excimer emission of **L** is directed by the coordination of the metal cation added first.

As summarized in Table 3, the lifetimes of the monomer and excimer emissions also depend on the input sequence. In the $Zn^{2+} \rightarrow Cd^{2+}$ sequence, $Cd^{2+}$ addition shortens the lifetimes of both emissions (monomer, 8.4→8.0 ns; excimer, 39.0→37.1 ns). This is because $Cd^{2+}$ coordination with **L** destabilizes the excited monomer and excimer due to formation of the $Cd^{2+}$–AN π complex. In contrast, in the $Cd^{2+} \rightarrow Zn^{2+}$ sequence, $Zn^{2+}$ addition lengthens the lifetime of the monomer emission (7.9→10.0 ns). This monomer lifetime is longer than those of all other complexes (< 8.4 ns), although the first $Cd^{2+}$ coordination may destabilize the excited monomer by formation of the strong $Cd^{2+}$–AN π complex. As shown in Table 4, the distances between the 10–10′ positions of the AN fragments of the [ZnL(OH)]$^+$ and [CdL(OH)]$^+$ complexes are 7.33 and 7.75 Å, respectively. This means that

the metal-free (vacant) polyamine ligand of $[CdL(OH)]^+$ has a metal-binding space larger than that of $[ZnL(OH)]^+$; in other words, the vacant polyamine ligand of $[CdL(OH)]^+$ can coordinate with metal cations more flexibly. This is because the coordination of $Cd^{2+}$, of larger ionic radius (1.10 Å) than $Zn^{2+}$ (0.74 Å),[24] pulls the bipolar AN fragments apart. The vacant polyamine ligand of $[CdL(OH)]^+$, therefore, coordinates with $Zn^{2+}$, of smaller ionic radius than $Cd^{2+}$, more strongly. This probably leads to an efficient suppression of ET from the nitrogen atoms of the ligand to the excited AN, thus lengthening the lifetime of the monomer emission.

## Conclusion

The emission properties of an azamacrocyclic ligand (**L**) containing two AN fragments have been studied in water. We found that **L** acts as the first fluorescent molecular switch driven by the input sequence of metal cations ($Zn^{2+}$ and $Cd^{2+}$). The basic concept presented here, which cleverly controls excimer emission by simple polyamine ligand and metal cation inputs, may contribute to the development of more miniaturized and more integrated fluorescent molecular devices.

## Experimental Section

**General**: All of the reagents used were of the highest commercial quality, and were supplied by Wako and Tokyo Kasei and used without further purification. Water was purified by the Milli Q system.

**Azamacrocyclic ligand L**: Anthracene-9,10-dicarbaldehyde (0.54 g, 2.3 mmol) and triethylenetetramine (0.37 g, 2.5 mmol) were stirred in a mixture of $CH_3CN$ and $CH_3OH$ (60:40 mL/mL) at 323 K under dry $N_2$. After 50 h of stirring, the solvents were removed by evaporation. $CH_3OH$ (50 mL) was added to the residue, and $NaBH_4$ (0.57 g, 15 mmol) was added carefully. After 12 h of stirring at 323 K, the solvents were removed by evaporation. Water (40 mL) and $CH_2Cl_2$ (90 mL) were added to the residue, and the resulting organic layer was dried over $Na_2SO_4$ and concentrated by evaporation. The semisolid residue obtained was dissolved in ethanol and precipitated as the HCl salt by addition of concentrated aqueous HCl solution. The salt was recrystallized in diethyl ether/ethanol, affording **L** as a brown powder (0.45 g, 20%). $^1$H NMR (270 MHz, $D_2O$, TMS): $\delta = 3.11–3.57$ (m, 24H; $CH_2$, polyamine), 5.46 (s, 8H; Ar$CH_2$), 7.82–8.46 ppm (m, 16H; Ar$H$); $^{13}$C NMR (270 MHz, $D_2O$, TMS): $\delta = 130.7, 128.6, 124.7, 123.8, 45.5, 44.4, 44.1$ ppm; FAB-MS: $m/z$: calcd for $C_{44}H_{56}N_8$: 696.46; found: 697.8 $[M+H^+]$.

**Analysis**: Steady-state fluorescence spectra were measured on a Hitachi F-4500 fluorescence spectrophotometer.[25] Absorption spectra were measured on a UV/Vis photodiode-array spectrophotometer (Shimadzu; Multispec-1500).[26] Time-resolved fluorescence decay measurements were performed by time-correlated single photon counting on a PTI-3000 apparatus (Photon Technology International) by using a Xe nanoflash lamp filled with $N_2$ as excitation source. All of the measurements were carried out in the presence of $NaClO_4$ to maintain the ionic strength of the solution ($I = 0.15$ M) and at $298 \pm 1$ K by using a quartz cell with 10 mm path length. The measurements in the presence of metal cations were carried out after adding a metal cation followed by stirring for 5 min, because >5 min stirring does not lead to any change in the spectra. For reproduction of the data, all of the measurements were carried out in aerated conditions. Potentiometric titrations were carried out on a

COMTITE-550 potentiometric automatic titrator (Hiranuma) with a glass electrode (GE-101).[27] An aqueous solution (50 mL) with an ionic strength of $I = 0.15$ ($NaClO_4$) containing **L** (0.01 mmol) with or without metal cation was kept under dry argon. At least two independent titrations were performed at $298 \pm 1$ K with an aqueous NaOH solution (0.35 mM). The protonation and intrinsic complexation constants of **L** were determined by the nonlinear least-squares program HYPERQUAD, for which the $K_w$ $(=[H^+][OH^-])$ value used was $10^{-13.73}$ at 298 K.[28] The stepwise protonation constants for **L** and stability constants for interaction between **L** and metal cations are summarized in Tables 1 and 2, respectively. $^1$H and $^{13}$C NMR spectra were obtained by a JEOL JNM-GSX270 Excalibur spectrometer with tetramethylsilane (TMS) as standard. FAB-MS spectra were obtained by a JEOL JMS-700 mass spectrometer. Semiempirical MO calculations were performed by the [D]MNDO method within the WinMOPAC version 3.0 software (Fujitsu).[29]

[1] a) V. Balzani, *Molecular Devices and Machines: A Journey into the Nano World*, Wiley-VCH, Weinheim, **2003**; b) B. L. Feringa, *Molecular Switches*, Wiley-VCH, Weinheim, **2001**; c) V. Balzani, A. Credi, F. M. Raymo, J. F. Stoddart, *Angew. Chem.* **2000**, *112*, 3484–3530; *Angew. Chem. Int. Ed.* **2000**, *39*, 3348–3391; d) C. P. Collier, E. W. Wong, M. Belohradsky, F. M. Raymo, J. F. Stoddart, P. J. Kuekes, R. S. Williams, J. R. Heath, *Science* **1999**, *285*, 391–394.

[2] a) Special Issue: *Photochromism: Memories and Switches* (Ed.: M. Irie), *Chem. Rev.* **2000**, *100*, 1683–1890; b) V. Amendola, L. Fabbrizzi, F. Foti, M. Licchelli, C. Mangano, P. Pallavicini, A. Poggi, D. Sacchi, A. Taglietti, *Coord. Chem. Rev.* **2006**, *250*, 273–299; c) F. M. Raymo, M. Tomasulo, *Chem. Eur. J.* **2006**, *12*, 3186–3193; d) G. Jiang, S. Wang, W. Yuan, L. Jiang, Y. Song, H. Tian, D. Zhu, *Chem. Mater.* **2006**, *18*, 235–237; e) C. Trieflinger, H. Röhr, K. Rurack, J. Daub, *Angew. Chem.* **2005**, *117*, 7104–7107; *Angew. Chem. Int. Ed.* **2005**, *44*, 6943–6947; f) C. M. Rudzinski, D. G. Nocera in *Optical Sensors and Switches* (Ed.: K. S. Schanze), Marcel Dekker, New York, **2001**, pp. 1–99.

[3] a) A. P. de Silva, H. Q. N. Gunaratne, T. Gunnlaugsson, A. J. M. Huxley, C. P. McCoy, J. T. Rademacher, T. E. Rice, *Chem. Rev.* **1997**, *97*, 1515–1566; b) L. Fabbrizzi, M. Licchelli, P. Pallavicini, *Acc. Chem. Res.* **1999**, *32*, 846–853; c) R. Martínez, I. Ratera, A. Tárraga, P. Molina, J. Veciana, *Chem. Commun.* **2006**, 3809–3811; d) D. A. Leigh, M. Á. F. Morales, E. M. Pérez, J. K. Y. Wong, C. G. Saiz, A. M. Z. Slawin, A. J. Carmichael, D. M. Haddleton, A. M. Brouwer, W. J. Buma, G. W. H. Wurpel, S. León, F. Zerbetto, *Angew. Chem.* **2005**, *117*, 3122–3127; *Angew. Chem. Int. Ed.* **2005**, *44*, 3062–3067.

[4] a) S. Uchiyama, N. Kawai, A. P. de Silva, K. Iwai, *J. Am. Chem. Soc.* **2004**, *126*, 3032–3033; b) N. Chandrasekharan, L. A. Kelly, *J. Am. Chem. Soc.* **2001**, *123*, 9898–9899; c) J. Lou, T. A. Hatton, P. E. Laibinis, *Anal. Chem.* **1997**, *69*, 1262–1264.

[5] a) L. Gobbi, P. Seiler, F. Diederich, *Angew. Chem.* **1999**, *111*, 737–740; *Angew. Chem. Int. Ed.* **1999**, *38*, 674–678; b) A. Beyeler, P. Belser, L. De Cola, *Angew. Chem.* **1997**, *109*, 2878–2881; *Angew. Chem. Int. Ed. Engl.* **1997**, *36*, 2779–2781; c) F. M. Raymo, M. Tomasulo, *J. Phys. Chem. A* **2005**, *109*, 7343–7352.

[6] a) L. Fabbrizzi, M. Licchelli, S. Mascheroni, A. Poggi, D. Sacchi, M. Zema, *Inorg. Chem.* **2002**, *41*, 6129–6136; b) G. Zhang, D. Zhang, X. Guo, D. Zhu, *Org. Lett.* **2004**, *6*, 1209–1212; c) P. Yan, M. W.

Holman, P. Robustelli, A. Chowdhury, F. I. Ishak, D. M. Adams, *J. Phys. Chem. B* **2005**, *109*, 130–137.

[7] a) A. P. de Silva, H. Q. N. Gunaratne, C. P. McCoy, *J. Am. Chem. Soc.* **1997**, *119*, 7891–7892; b) S. A. de Silva, B. Amorelli, D. C. Isidor, K. C. Loo, K. E. Crooker, Y. E. Pena, *Chem. Commun.* **2002**, 1360–1361; c) M. T. Albelda, M. A. Bernardo, P. Díaz, E. García-España, J. Seixas de Melo, F. Pina, C. Soriano, S. V. Luis, *Chem. Commun.* **2001**, 1520–1521.

[8] a) A. P. de Silva, D. B. Fox, A. J. M. Huxley, T. S. Moody, *Coord. Chem. Rev.* **2000**, *205*, 41–57; b) L. Fabbrizzi, M. Licchelli, P. Pallavicini, A. Taglietti, *Inorg. Chem.* **1996**, *35*, 1733–1736.

[9] a) B. Valeur, I. Leray, *Coord. Chem. Rev.* **2000**, *205*, 3–40; b) J.-S. Yang, Y.-D. Lin, Y.-H. Chang, S.-S. Wang, *J. Org. Chem.* **2005**, *70*, 6066–6073.

[10] a) D. Margulies, G. Melman, C. E. Felder, R. Arad-Yellin, A. Shanzer, *J. Am. Chem. Soc.* **2004**, *126*, 15400–15401; b) M. T. Albelda, P. Díaz, E. García-España, J. C. Lima, C. Lodeiro, J. Seixas de Melo, A. J. Parola, F. Pina, C. Soriano, *Chem. Phys. Lett.* **2002**, *353*, 63–68.

[11] a) R.-H. Yang, W.-H. Chan, A. W. M. Lee, P.-F. Xia, H.-K. Zhang, K. Li, *J. Am. Chem. Soc.* **2003**, *125*, 2884–2885; b) B. Bodenant, F. Fages, M.-H. Delville, *J. Am. Chem. Soc.* **1998**, *120*, 7511–7519; c) E. M. Nolan, S. J. Lippard, *J. Am. Chem. Soc.* **2003**, *125*, 14270–14271; d) J. F. Callan, A. P. de Silva, N. D. McClenaghan, *Chem. Commun.* **2004**, 2048–2049; e) B. Bag, P. K. Bharadwaj, *Org. Lett.* **2005**, *7*, 1573–1576.

[12] a) S. K. Kim, S. H. Lee, J. Y. Lee, J. Y. Lee, R. A. Bartsch, J. S. Kim, *J. Am. Chem. Soc.* **2004**, *126*, 16499–16506; b) J.-M. Montenegro, E. Perez-Inestrosa, D. Collado, Y. Vida, R. Suau, *Org. Lett.* **2004**, *6*, 2353–2355; c) D. Marquis, J.-P. Desvergne, H. Bouas-Laurent, *J. Org. Chem.* **1995**, *60*, 7984–7996; d) G. McSkimming, J. H. R. Tucker, H. Bouas-Laurent, J.-P. Desvergne, S. J. Coles, M. B. Hursthouse, M. E. Light, *Chem. Eur. J.* **2002**, *8*, 3331–3342; e) A. Ajayaghosh, P. Carol, S. Sreejith, *J. Am. Chem. Soc.* **2005**, *127*, 14962–14963; f) P. Ghosh, P. K. Bharadwaj, S. Mandal, S. Ghosh, *J. Am. Chem. Soc.* **1996**, *118*, 1553–1554.

[13] L. Fabbrizzi, M. Licchelli, N. Marcotte, F. Stomeo, A. Taglietti, *Supramol. Chem.* **2002**, *14*, 127–132.

[14] a) Y. Shiraishi, Y. Tokitoh, G. Nishimura, T. Hirai, *Org. Lett.* **2005**, *7*, 2611–2614; b) G. Nishimura, Y. Shiraishi, T. Hirai, *Chem. Commun.* **2005**, 5313–5315.

[15] a) E. U. Akkaya, M. E. Huston, A. W. Czarnik, *J. Am. Chem. Soc.* **1990**, *112*, 3590–3593; b) S. Alves, F. Pina, M. T. Albelda, E. García-España, C. Soriano, S. V. Luis, *Eur. J. Inorg. Chem.* **2001**, 405–412.

[16] a) H. Wadepohl, *Angew. Chem.* **1992**, *104*, 253–268; *Angew. Chem. Int. Ed. Engl.* **1992**, *31*, 247–262; b) J. C. Ma, D. A. Dougherty, *Chem. Rev.* **1997**, *97*, 1303–1324; c) A. Ikeda, S. Shinkai, *Chem. Rev.* **1997**, *97*, 1713–1734; d) A. Ikeda, S. Shinkai, *J. Am. Chem. Soc.* **1994**, *116*, 3102–3110.

[17] a) Y. Shiraishi, Y. Tokitoh, T. Hirai, *Chem. Commun.* **2005**, 5316–5318; b) T. Gunnlaugsson, T. C. Lee, R. Parkesh, *Tetrahedron* **2004**, *60*, 11239–11249.

[18] a) Y. Shiraishi, Y. Kohno, T. Hirai, *J. Phys. Chem. B* **2005**, *109*, 19139–19147; b) M. E. Huston, C. Engleman, A. W. Czarnik, *J. Am. Chem. Soc.* **1990**, *112*, 7054–7056.

[19] L. Pauling, *The Nature of the Chemical Bond*, 3rd ed., Cornell University Press, New York, **1960**.

[20] a) Y. Shiraishi, Y. Tokitoh, T. Hirai, *Org. Lett.* **2006**, *8*, 3841–3844; b) Y. Shiraishi, Y. Tokitoh, G. Nishimura, T. Hirai, *J. Phys. Chem. B* **2007**, *111*, 5090–5100; c) J.-S. Yang, C.-S. Lin, C.-Y. Hwang, *Org. Lett.* **2001**, *3*, 889–892; d) H. J. Kim, S. K. Kim, J. Y. Lee, J. S. Kim, *J. Org. Chem.* **2006**, *71*, 6611–6614; e) Y. Shiraishi, K. Ishizumi, G. Nishimura, T. Hirai, *J. Phys. Chem. B* **2007**, *111*, 8812–8822.

[21] a) C. Bazzicalupi, A. Bencini, A. Bianchi, C. Giorgi, V. Fusi, B. Valtancoli, M. A. Bernardo, F. Pina, *Inorg. Chem.* **1999**, *38*, 3806–3813; b) M. A. Bernardo, F. Pina, E. García-España, J. Latorre, S. V. Luis, J. M. Llinares, J. A. Ramírez, C. Soriano, *Inorg. Chem.* **1998**, *37*, 3935–3942; c) M. A. Bernardo, F. Pina, B. Escuder, E. García-España, M. L. Godino-Salido, J. Latorre, S. V. Luis, J. A. Ramírez, C. Soriano, *J. Chem. Soc. Dalton Trans.* **1999**, 915–921.

[22] a) X. Guo, D. Zhang, T. Wang, D. Zhu, *Chem. Commun.* **2003**, 914–915; b) J. Kawakami, T. Niiyama, S. Ito, *Anal. Sci.* **2002**, *18*, 735–736.

[23] M. Eigen, R. G. Wilkins, *Mechanisms of Inorganic Reactions, Advances in Chemistry, Vol. 49* (Ed.: R. F. Gould), ACS, Washington, DC, **1965**.

[24] C. A. Chang, V. O. Ochaya, *Inorg. Chem.* **1986**, *25*, 355–358.

[25] a) Y. Shiraishi, M. Morishita, Y. Teshima, T. Hirai, *J. Phys. Chem. B* **2006**, *110*, 6587–6594; b) M. Morishita, Y. Shiraishi, T. Hirai, *J. Phys. Chem. B* **2006**, *110*, 17898–17905.

[26] a) H. Koizumi, Y. Shiraishi, S. Tojo, M. Fujitsuka, T. Majima, T. Hirai, *J. Am. Chem. Soc.* **2006**, *128*, 8751–8753; b) Y. Shiraishi, H. Koizumi, T. Hirai, *J. Phys. Chem. B* **2005**, *109*, 8580–8586; c) Y. Shiraishi, M. Morishita, T. Hirai, *Chem. Commun.* **2005**, 5977–5979.

[27] G. Nishimura, K. Ishizumi, Y. Shiraishi, T. Hirai, *J. Phys. Chem. B* **2006**, *110*, 21596–21602.

[28] A. Sabatini, A. Vacca, P. Gans, *Coord. Chem. Rev.* **1992**, *92*, 389–405.

[29] a) Y. Shiraishi, N. Saito, T. Hirai, *J. Am. Chem. Soc.* **2005**, *127*, 8304–8306; b) Y. Shiraishi, N. Saito, T. Hirai, *J. Am. Chem. Soc.* **2005**, *127*, 12820–12822; c) Y. Shiraishi, N. Saito, T. Hirai, *Chem. Commun.* **2006**, 773–775.